



OPEN

# A 338-year tree-ring oxygen isotope record from Thai teak captures the variations in the Asian summer monsoon system

Nathsuda Pumijumnong<sup>1</sup>, Achim Bräuning<sup>2</sup>, Masaki Sano<sup>3</sup>, Takeshi Nakatsuka<sup>4</sup>, Chotika Muangsong<sup>5</sup> ✉ & Supaporn Buajan<sup>1</sup>

A 338-year oxygen isotope record from teak tree-ring cellulose collected from Mae Hong Son province in northwestern Thailand was presented. The tree-ring series preserves the isotopic signal of the regional wet season rainfall and relative humidity. Tree-ring  $\delta^{18}\text{O}$  correlates strongly with regional rainfall from May to October, showing coherent variations over large areas in Southeast Asia. We reconstructed the summer monsoon season (May to October) rainfall based on a linear regression model that explained 35.2% of the actual rainfall variance. Additionally, we found that in the 19<sup>th</sup> century, there was a remarkable drought during many years that corresponded to regional historic drought events. The signals of the June to September Indian summer monsoon (ISM) for the period between 1948 and 2009 were clearly found. Spatial correlations and spectral analyses revealed a strong impact of the El Niño–Southern Oscillation (ENSO) on tree-ring  $\delta^{18}\text{O}$ . However, ENSO influenced the tree-ring  $\delta^{18}\text{O}$  more strongly in the 1870–1906, 1907–1943, and 1944–1980 periods than in the 1981–2015 period, which corresponded to periods of weaker and stronger ISM intensity.

The Asian summer monsoon (ASM) is an important component of global monsoons and is one of the dominant summer rainfall regimes in the world. Changes in ASM activity have strong implications for the economy and livelihood of more than two billion people, which are directly or indirectly affected by the timing and amount of precipitation during the ASM season<sup>1</sup>. Therefore, understanding climate change and climate variability effects on the ASM is highly relevant. However, a clearer understanding of long-term monsoon variability is hampered by the scarcity of long instrumental climate records for the tropics. Thus, climate proxy records are needed to extend the existing instrumental climate series into the past to learn more about the long-term natural variability in the ASM and to analyze the recent climate change trends.

Thailand, a country located in tropical Southeast Asia, is governed by the ASM climate. The economy and environment of the region strongly depend on climatic conditions. Asian and Southeast Asian countries are home to a large population and are important global food producers<sup>2</sup>. As such, climate change could affect the intensity and frequency of rainfall patterns, which could seriously impact food production.

Among other climate proxies, tree rings have the advantages of an annual resolution and precise dating control<sup>3</sup>. One restriction pertaining to dendrochronological studies within the Southeast Asian region is the scarcity of tree species that produce clear annual growth rings. Although a number of tree species in South Asia have recently been found to produce annual tree rings and can produce tree-ring chronologies that are useful for climate reconstruction<sup>4</sup>, mostly teak (*Tectona grandis*, L.f), they have so far been successfully used to produce long tree-ring chronologies used for climate reconstructions from the Asian tropics due to their wide distribution; teak was also been used as construction timber in historical buildings. However, previous studies<sup>5–9</sup> provided climate reconstructions based on teak tree-ring records, which did not pass some verification tests. As an alternative

<sup>1</sup>Faculty of Environment and Resource Studies, Mahidol University, Mahidol, Thailand. <sup>2</sup>Institute of Geography, Friedrich-Alexander University Erlangen-Nürnberg, Erlangen-Nürnberg, Germany. <sup>3</sup>Faculty of Human Sciences, Waseda University, Tokorozawa, Japan. <sup>4</sup>Nagoya University, Nagoya, Japan. <sup>5</sup>Innovation for Social and Environmental Management, Mahidol University, Amnatcharoen Campus, Amnatcharoen, Thailand. ✉e-mail: [chotika.mua@mahidol.ac.th](mailto:chotika.mua@mahidol.ac.th)

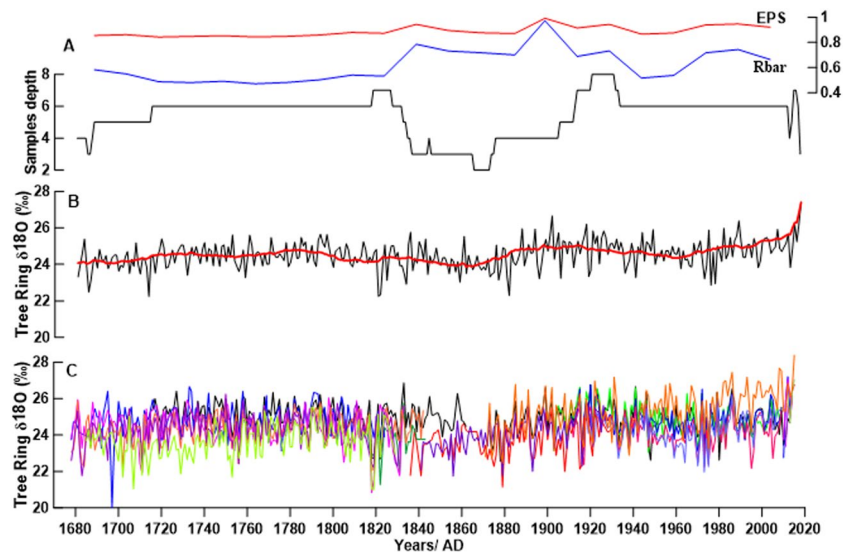


**Figure 1.** Sample depth, running EPS, and Rbar statistics of the mean isotope chronology (A) Thai teak tree-ring  $\delta^{18}\text{O}$  chronology (black line), 11-year low pass filter (red line) (B), and individual teak tree-ring  $\delta^{18}\text{O}$  series (C).

method, stable isotopes in tree rings have been examined worldwide, especially in tropical regions<sup>10–12</sup> to gain information about variations in the hydrological system<sup>13</sup>.

To this end, the oxygen isotope ratios ( $\delta^{18}\text{O}$ ) in tree-ring cellulose are increasingly being used as a tool to obtain retrospective insights into ecophysiological processes<sup>14</sup>. One advantage of using the  $\delta^{18}\text{O}$  in tree-ring cellulose compared to tree ring width is that  $\delta^{18}\text{O}$  lacks internal trends related to juvenile effects<sup>15</sup>. In addition, tree-ring  $\delta^{18}\text{O}$  first reflects the isotopic composition of the source water, which is then altered by leaf enrichment<sup>16</sup>.

Hence,  $\delta^{18}\text{O}$  in tree-ring cellulose can provide insights into the causes behind the variations in moisture sources<sup>17,18</sup>. Existing tree-ring stable oxygen isotope studies in temperate climate zones are numerous<sup>19–21</sup>. The study of oxygen isotopes in tropical regions in South America is still more abundant than those in Southeast Asia, such as Costa Rica<sup>11,12</sup>, and in Bolivia<sup>13</sup>, the number of existing tree-ring studies using stable isotopes within Southeast Asia remains small<sup>22–25</sup>. This lack of studies is partly due to the lack of suitable, old specimens but also due to the lagged development in terms of tropical dendroecological discoveries of new tree species suitable for tree-ring studies. In this study, we produced the longest oxygen isotope chronology currently available from tree-ring cellulose of teak and examined the influence of local and regional climate parameters on oxygen isotope ratios ( $\delta^{18}\text{O}$ ) to improve our understanding of ASM variability during the past 338 years.

## Results

**Teak tree-ring  $\delta^{18}\text{O}$  ( $\delta^{18}\text{O}_{\text{tr}}$ ) chronology.** Results indicated significant intercorrelations for the most of the individual tree-ring  $\delta^{18}\text{O}$  ( $\delta^{18}\text{O}_{\text{tr}}$ ) series and permitted for calculating the mean regional site chronology. Figure 1 shows the annually resolved  $\delta^{18}\text{O}_{\text{tr}}$  mean values of tree-ring cellulose from 21 trees for the period AD 1678–2015 along with the running expressed population signal (EPS) and inter-series correlation (Rbar) statistics, through the use of 30-year windows, and when lagged 15 years (Fig. 1). The Rbar statistic for these data spans a range of 0.4–0.81, and EPS is in the range of 0.7–0.95. For our  $\delta^{18}\text{O}_{\text{tr}}$  series, the EPS value of  $\geq 0.85$  is generally accepted but fell below this criterion is associated with diminished the sample size.<sup>26</sup> Buras<sup>27</sup> explained that EPS indicates how good a finite sample of tree-ring data is for an infinite population. Therefore, values that are lower than 0.85 do not mean that the chronology is unreliable. Due to the tree-ring  $\delta^{18}\text{O}$  study, the number of samples taken is not as high as those for the tree ring width study. Therefore, at some times, an EPS value lower than 0.85 does not mean that the value is unreliable. Teak  $\delta^{18}\text{O}_{\text{tr}}$  values ranged between 20.81 and 26.90‰, and the long-term average was 24.44‰.

**Teak  $\delta^{18}\text{O}_{\text{tr}}$  and local and regional climate data.** Figure 2 shows the relationship among  $\delta^{18}\text{O}_{\text{tr}}$  and rainfall, humidity, and temperature at the Mae Hong Son meteorological station (hereinafter named the local climate),  $\delta^{18}\text{O}_{\text{rain}}$  at Bangkok Station and CRU T4.03 rainfall and temperature (hereinafter named the regional climate). The  $\delta^{18}\text{O}_{\text{tr}}$  has a negative correlation with the local rainfall (May–October (M–O),  $r = -0.413$ ,  $p < 0.001$ ), local humidity (May–June–July (MJJ),  $r = -0.439$ ,  $p < 0.001$ ) and regional rainfall (M–O,  $r = -0.593$ ,  $p < 0.001$ ).

A spatial correlation analysis was performed to demonstrate the relationship between  $\delta^{18}\text{O}_{\text{tr}}$  and the amount of precipitation in the tropics. Regions showing significant negative correlations with the  $\delta^{18}\text{O}_{\text{tr}}$  series appeared over wide areas in Southeast Asia as well as in the eastern parts of the Indian subcontinent. The correlation was strongest over northwestern Thailand and decreased toward the east (Fig. 3).

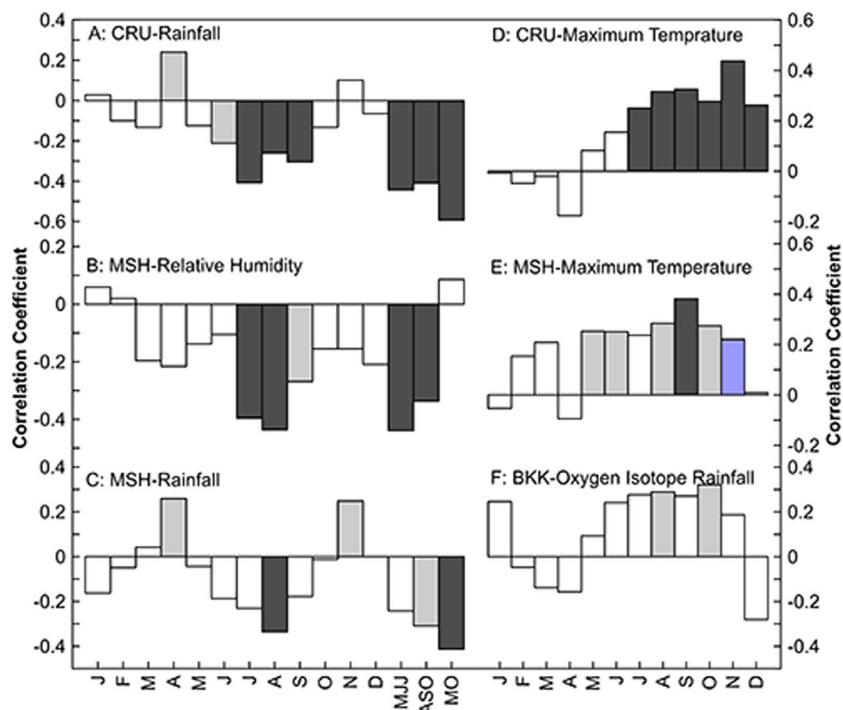


**Figure 2.** Correlations between tree-ring  $\delta^{18}\text{O}$  and rainfall obtained from the CRU TS4.03 during the period 1901–2015 (A), relative humidity (%) obtained from the Mae Hong Son meteorological station during the period 1950–2015 (B), rainfall obtained from the Mae Hong Son instrumental station during the period 1911–2015 (C), mean maximum temperature obtained from the CRU TS4.03 during the period of 1901–2015 (D), mean maximum temperature at Mae Hong Son meteorologica station during the period of 1951–2015 (E), and  $\delta^{18}\text{O}$  in rainfall in Bangkok (F). Black bars indicate correlations that are significant at the 99% level of confidence; light blue bars indicate correlations significant at the 95% level of confidence.

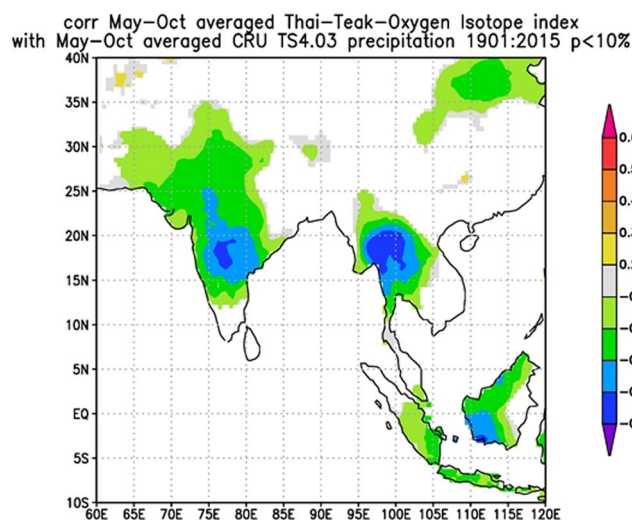


**Figure 3.** Spatial correlation pattern of Thai Teak  $\delta^{18}\text{O}_{\text{tr}}$  vs. CRU TS4.03 May–October precipitation.

**Teak  $\delta^{18}\text{O}_{\text{tr}}$  and monsoon indices.** The significant negative relationship between  $\delta^{18}\text{O}_{\text{tr}}$  and ISM and the Webster and Yang Monsoon Index (WYM) was highest from June to August (JJA) ( $r = -0.544$ ,  $p < 0.001$ ) and highest from June to September (JJAS) ( $r = -0.459$ ,  $p < 0.001$ ) (data not shown).

**Spectral analyses.** The spectral analysis revealed significant peaks ( $p < 0.01$ ) at years 100, 4 and 2 (Fig. S1) for cyclicity. Notably, short cycles of 4–7 years correspond to the typical ENSO frequency band. The significant periodicity band with a frequency of 100 years may be related to the Pacific Multidecadal Oscillation<sup>28</sup> and long-term summer monsoon variability<sup>29</sup>.

Calibration				Verification				RE	CE
Period	r	r <sup>2</sup>	ST	period	r	r <sup>2</sup>	ST		
1904–1959	0.514	0.264	36/–20	1960–2015	0.643	0.413	35/–21	0.386	0.385
1960–2015	0.643	0.413	37/–19	1904–1959	0.514	0.264	35/–21	0.229	0.227
1904–2015	0.593	0.352	72/–40						

**Table 1.** Calibration and verification of May to October precipitation reconstruction. ST = sign test, RE = reduction of error, CE = coefficient of efficiency Significant level at  $p < 0.05$  level Figures and captions:

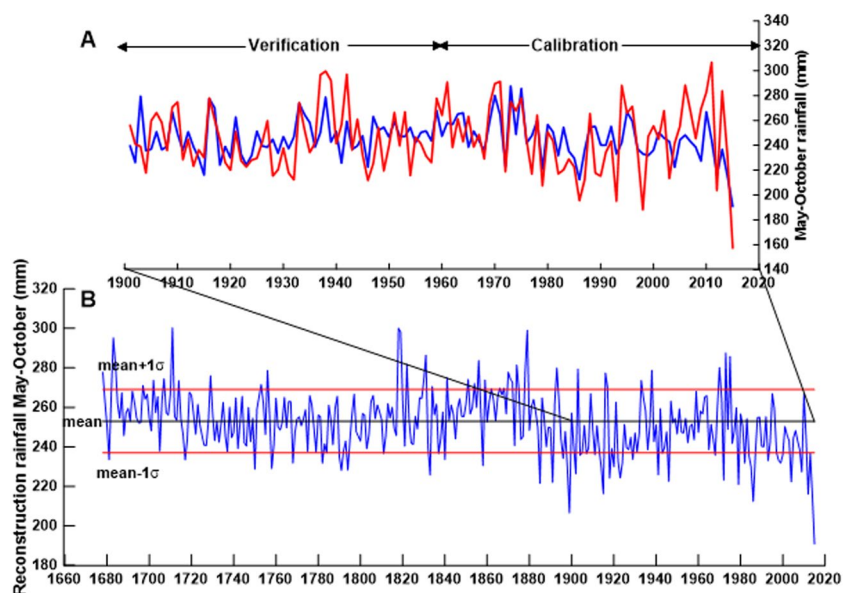


**Figure 4.** May to October rainfall (mm), red line is actual CRU TS4.03 rainfall (mm) and blue line is reconstruction May–October rainfall (mm) (A), reconstruction rainfall May–October black line is the average rainfall of 253 mm, read line (mean +  $1\sigma$ ) is 269 mm, and (mean –  $1\sigma$ ) is 237 mm (B).

**Global correlation between  $\delta^{18}\text{O}_{\text{tr}}$  and sea surface temperature.** We found significant positive relationships between our  $\delta^{18}\text{O}_{\text{tr}}$  and the multivariate ENSO index (MEI). Correlations with the extended multivariate ENSO index (MEI\_ext range of 1871–2005) were similar to MEI, in which the relationship began in May, with September showing the highest positive correlation ( $r = 0.565$ ,  $p < 0.001$ ). The same relationship was found between  $\delta^{18}\text{O}_{\text{tr}}$  and both Niño3.4 and Niño4, with the highest positive correlation occurring in October for Niño4 ( $r = 0.577$ ,  $p < 0.001$ ) (Fig. S2). Correlations between  $\delta^{18}\text{O}_{\text{tr}}$  and Dipole Mode Index (DMI) over the entire period (1870–2015) revealed significant positive relationships from June to October, with October being the month that had the highest correlation ( $r = 0.453$ ,  $p < 0.001$ ). Furthermore, a positive relationship between  $\delta^{18}\text{O}_{\text{tr}}$  and Pacific Decadal Oscillation (PDO) is found from July to December, with the highest correlation in August ( $r = 0.258$ ,  $p < 0.005$ ). Our  $\delta^{18}\text{O}_{\text{tr}}$  and Palmer Drought Severity Index (PDSI) showed significant negative correlations over the whole year, with the highest correlations being from October to December ( $r = -0.449$ ,  $p < 0.001$ ).

**Reconstruction of May to October (M–O) rainfall.** The correlation between  $\delta^{18}\text{O}_{\text{tr}}$  and regional climate precipitation of M–O showed the highest value ( $r = -0.593$ ,  $p < 0.001$ ); therefore, precipitation during the ASM season was targeted for climate reconstruction. We used a simple regression model to develop a transfer function, which is shown as follows:  $P_{\text{MO}} = 772.985 + (-21.250) * \delta^{18}\text{O}_{\text{tr}}$ , where  $P_{\text{MO}}$  represents May–October rainfall. We divided this period into two subperiods, 1904–1959 and 1960–2015, for crosswise calibration and verification. The verification and calibration statistics are shown in Table 1. The values for Reduction of Error (RE) and Coefficient of Efficiency (CE) are positive in both subperiods, indicating the validity of the oxygen isotope record as a climate estimate<sup>30</sup>. Finally, we reconstructed the precipitation from May–October based on the full dataset for calibration. The linear regression model explained 35.20% of the actual variance in the May–October precipitation (Fig. 4).

## Discussion and conclusions

**Teak oxygen isotope chronology characteristics.** A 338-year-long teak oxygen isotope chronology for the period of AD 1678–2015 was developed, including data from 21 individual living teak trees from the Mae Hong Son Province, northwest Thailand. Instead of pooling the tree-ring material from several trees as mentioned above, we constructed the chronology by averaging the isotope series from individual trees that were well intercorrelated, allowing precise dating control on all individual  $\delta^{18}\text{O}_{\text{tr}}$  values. For this approach, our chronology

is covered by at least 4 trees after 1680; however, there is one particular period (ca. 1860–1870) where the chronology shows low replication. It is possible that the period was one of the heavy teak concessions, so old trees did not remain (Fig. 1).

**Possible mechanisms for the strong precipitation signal in  $\delta^{18}\text{O}_{\text{tr}}$ .** Our  $\delta^{18}\text{O}_{\text{tr}}$  chronology exhibits a stable inverse relationship with the local and regional rainy season (May to October) precipitation ( $r = -0.413$ ,  $p < 0.001$ ,  $n = 65$  and  $r = -0.593$ ,  $p < 0.001$ ,  $n = 112$ , respectively), probably as a result of the well-known “amount effect”<sup>31</sup>, and a positive relationship with the maximum temperature from June to December (highest in November,  $r = 0.437$ ,  $p < 0.001$ ,  $n = 112$ ) during the dry season. It is possible that the source water signal of the soil is dominated by seasonally changing  $\delta^{18}\text{O}$  signatures in precipitation. As our study trees grew on mountain slopes, any groundwater impact on the tree-ring oxygen isotope signature can be excluded. In addition, teak has a shallow root system<sup>32</sup> and grows well on well-drained soils. Thus, variations in oxygen isotope series in teak wood are expected to reflect the variations in oxygen isotope ratios in seasonal rainfall, which is affirmed by the significant positive correlation between  $\delta^{18}\text{O}_{\text{tr}}$  and annual  $\delta^{18}\text{O}$  in rainfall from the Global Network of Isotopes in Precipitation (GNIP) station in Bangkok (August  $r = 0.289$ ,  $p < 0.045$ ,  $n = 48$ , October  $r = 0.321$ ,  $p < 0.030$ ,  $n = 46$ ). Duy *et al.*<sup>33</sup> concluded that the variation in oxygen isotopes in rainwater is 70% controlled by regional moisture regimes compared to local climatic conditions (30%), and regional and local factors vary in importance seasonally and have a large influence on the isotopic composition of rainfall. According to our results, local rainfall and regional rainfall are related to  $\delta^{18}\text{O}_{\text{tr}}$  in the same direction, and seasonal rainfall quite clearly controls the signature in  $\delta^{18}\text{O}_{\text{tr}}$ . However, it is also clear that local precipitation throughout the rainy season (MO) has less relation to  $\delta^{18}\text{O}_{\text{tr}}$  than regional rainfall. Rainfall in the Mae Hong Son Province is clearly influenced by the Indian Ocean at the beginning of the rainy season (MJJ) and by the South China Sea at the end of the rainy season (ASO). The results of this study have been confirmed by the studies of Cai *et al.*<sup>34</sup>, Muangsong *et al.*<sup>24</sup>, and Wei *et al.*<sup>35</sup>. We showed the moisture trajectory in May, which is the source of moisture from the Indian Ocean, in September, which is the source of moisture from the South China Sea (Fig. S3) and the wind vector from 1981–2010 during May to July, August to September, and November to December. It is clear that the direction of the wind changed from the beginning of the rainy season to the dry season (Fig. S4). However, the regional climate covers more extensive areas, which causes fluctuations in  $\delta^{18}\text{O}_{\text{rain}}$  and the enrichment of oxygen isotopes in leaves until they accumulate in trees. Therefore, it is found that regional rainwater throughout the rainy season is associated with higher  $\delta^{18}\text{O}_{\text{tr}}$  than local rainwater. Nevertheless, more research on the relationship of  $\delta^{18}\text{O}_{\text{rain}}$  and amount of rainfall in the regions influenced by the Asian monsoon pointed out that it was controlled by convective heat transfer and terrain<sup>36,37</sup>. Therefore, we find that not every month of rainfall is associated with  $\delta^{18}\text{O}_{\text{tr}}$ .

Furthermore, our results correspond to the studies of Brienen *et al.*<sup>13</sup> and Volland *et al.*<sup>38</sup>, which used  $\delta^{18}\text{O}_{\text{tr}}$  in tree rings of *Cedrela spp.* from the Amazon basin and its surroundings and found significant positive correlations between  $\delta^{18}\text{O}_{\text{tr}}$  and  $\delta^{18}\text{O}$  in rainfall. The climate signals captured by our isotope record also agree with the studies of Muangsong *et al.*<sup>24,25</sup> and Schollaen *et al.*<sup>23</sup>. During the transitional months from the end of the dry season to the beginning of the rainy season (April), teak cambium becomes active<sup>28</sup>. However, evaporation during this time of the year is high, leading to  $^{18}\text{O}$ -enriched leaf water. Hence, we found stronger correlations between  $\delta^{18}\text{O}_{\text{tr}}$  and air humidity (July, August, and September,  $r = -0.396$ ,  $p < 0.001$ ,  $n = 66$ ,  $r = -0.436$ ,  $p < 0.001$ ,  $n = 66$ ,  $r = -0.269$ ,  $p < 0.029$ ,  $n = 65$ ). Tree-ring  $\delta^{18}\text{O}$  values in this region are not only controlled by total (or annual) rainfall but also by monthly and seasonal rainfall isotopic signatures. Hence, dominant variations in monthly and/or seasonal inputs of rainwater isotope signals are related to different humidity sources, which can be assigned values of  $\delta^{18}\text{O}_{\text{tr}}$  in this region and may also result in different  $\delta^{18}\text{O}_{\text{tr}}$  values, which may be the same species<sup>39</sup> or trees that grow in nearby areas<sup>22,24</sup>. In addition, an important process affecting  $\delta^{18}\text{O}_{\text{tr}}$  is the fractionation of the oxygen isotope that occurs in leaves through the evapotranspiration process compliance with the maximum temperature control fluctuations in oxygen isotopes during warmer conditions, which enhances the evaporation of the soil water and increases  $\delta^{18}\text{O}$  in the source water<sup>40</sup>, resulting in the abundance of the leaf water isotope<sup>41</sup>.

**Comparison between  $\delta^{18}\text{O}_{\text{tr}}$  and other proxies in nearby areas.** The relationship between our teak  $\delta^{18}\text{O}_{\text{tr}}$  and teak  $\delta^{18}\text{O}_{\text{tr}}$  from the Phrae Province, which is approximately 400 km away, was  $0.501$ ,  $p < 0.001$ <sup>42</sup>, and Myanmar teak  $\delta^{18}\text{O}_{\text{tr}}$  was  $0.566$ ,  $p < 0.001$ <sup>43</sup>. We also found a relationship between our teak  $\delta^{18}\text{O}_{\text{tr}}$  and *Pinus merkusii*  $\delta^{18}\text{O}$  from Mae Hong Son ( $0.646$ ,  $p < 0.001$ )<sup>44</sup> and from Umpang, Tak Province ( $0.522$ ,  $p < 0.001$ )<sup>45</sup>. This correlation coefficient was higher than the correlation found with the *Pinus kesiya* oxygen isotope series studied by Zhu *et al.*<sup>46</sup>, indicating that there was a common moisture source for the studied teak and *Pinus merkusii* trees. This has important implications for further studies on stable oxygen isotopes for both species to extend the existing records. It is interesting because the *Fokienia hodginsii* tree-ring  $\delta^{18}\text{O}$  from Vietnam ( $r = 0.328$ ,  $p < 0.001$ )<sup>47</sup> and the same species from Laos ( $r = 0.174$ ,  $p < 0.005$ )<sup>48</sup> correlated with our teak  $\delta^{18}\text{O}_{\text{tr}}$ . The oxygen isotopes in tree rings are a great tool to study the hydrology cycle in Southeast Asia (Fig. S5).

In addition to the tree-ring  $\delta^{18}\text{O}$  that are extensively used in the study of monsoon dynamics, stalagmites in Thailand have also been studied for monsoon dynamics. We found that the teak  $\delta^{18}\text{O}_{\text{tr}}$  has a positive relationship with high-resolution oxygen isotope record of stalagmites from Klang Cave in southern Thailand<sup>49</sup> after running a 31-point smoothing filter ( $r = 0.328$ ,  $p < 0.001$ ) as well as growth rate profile, derived from stalagmite NJ-0901, from Nam Jang Cave in Mae Hong Son province of northwestern Thailand<sup>50</sup> based upon data smoothed with a 7-point running-average filter ( $r = 0.430$ ,  $p < 0.001$ ) (Fig. S6). Therefore, it is likely that we will gather proxies to be used to study the dynamics of the monsoon to unravel the complexity of the monsoon (Fig. S6).

**Reconstruction of summer precipitation during the past 338 years.** Our May to October precipitation reconstruction revealed that over the entire period from 1678–2015, summer precipitation in north-west Thailand had decreased, and the reconstructed long-term average of May–October (rainy season) average

precipitation was 253 mm. The dry period mean minus the standard deviation is equal to 237 mm, and the wet period mean plus the standard deviation is equal to 269 mm. We found that during the 17<sup>th</sup> and 18<sup>th</sup> centuries, drought occurred during 8 years, respectively. In the 19<sup>th</sup> century, there was drought during 19 years. In the 17<sup>th</sup>, 18<sup>th</sup>, and 19<sup>th</sup> centuries, wet years occurred during 6, 10 and 1 years, respectively. Our May–October rainfall reconstruction corresponds to the findings of Xu *et al.*<sup>44,45</sup> using pine tree-ring oxygen isotopes, from both the Mae Hong Son and Tak Provinces. It was found that during the 17<sup>th</sup> century, rainfall tended to decrease, and the drought period continued more often than during periods of heavy rainfall. The mechanism that may support drought in Southeast Asia is the southward shift in the Intertropical Convergence Zone (ITCZ). The results of the rainfall reconstruction using stalagmite  $\delta^{18}\text{O}$  from Klang Cave<sup>49</sup> found that the ITCZ has moved southward since the 18<sup>th</sup> century, and the most noticeable period is the 1980s.

In addition, our results are in line with the findings of Buckley *et al.*<sup>6</sup>, who built a teak growth index of living trees and stumps that covered 448 years. In particular, Buckley *et al.*<sup>6</sup> proposed a relationship between teak growth and PDSI and highlighted the drought that was recorded by the teak index in the early and mid-1700s. Our study also found a significantly negative correlation between the  $\delta^{18}\text{O}_{\text{tr}}$  of teak and PDSI, showing higher correlation coefficients than the teak ring width index. In addition, these findings are consistent with other reconstructed mega drought events, especially those found in the 18<sup>th</sup> century, such as the Strange Parallels drought (1756–1768) and the East India drought (1790–1796)<sup>51</sup>. Anderson *et al.*<sup>52</sup> found that during almost the entire 18<sup>th</sup> century, the weakening of the southwest monsoon was a result of cooler North Atlantic sea surface temperatures (SST).

**Large-scale drivers of interannual to decadal variations in tree-ring oxygen isotopes.** The significant positive relationships of our  $\delta^{18}\text{O}_{\text{tr}}$  with MEI (1950–2015), MEI extended (1871–2005), Niño3.4 (1870–2015) and Niño4 (1870–2005) point to a strong impact of ENSO on rainfall variability in northwest Thailand.

We calculated the relationships between  $\delta^{18}\text{O}_{\text{tr}}$  and Niño4 SSTs over different periods. During the four periods of 1870–1906, 1907–1943, 1944–1980, and 1981–2015,  $\delta^{18}\text{O}_{\text{tr}}$  and SSTs showed strong positive correlations. The most affected time was in the period of 1870–1906, the relationship between  $\delta^{18}\text{O}_{\text{tr}}$  and Niño4 shows a decrease in the positive relationship, and the month that appears to be somewhat delayed but is still significant is between 1981–2015. In general, the IM was strongly influenced by the ENSO during the first half of the 20<sup>th</sup> century, whereas since the 1980s, the IM has been increasingly influenced by the Indian Ocean Dipole (IOD)<sup>53</sup>. Pratarastapornkul<sup>54</sup> proposed that the IOD phenomenon affects annual rainfall in Thailand and that its impact varies depending on the combined effect and strength of the ENSO and IOD in the Pacific Ocean. As such, it is likely that excess rainfall and severe floods are to be expected in most regions of Thailand in cases of strong IOD events that combine with weak El Niño events.

The El Niño–Southern Oscillation (ENSO) is a major driver of global climate variability. The ENSO also interacts with other modes of climate variability, such as the Indian summer monsoon rainfall (ISMR). The easterly trade winds and SST gradients across the equatorial Pacific undergo a regime change, with enhanced trade winds and significant cooling (warming) over the tropical eastern (western) Pacific in the later period. Previous research has shown that the relationship between the ISRM and SSTs is variable<sup>55,56</sup>. The strongest relationships were found on short timescales (interdecadal periodicity, 2–7 years) or decadal periodicity (10.5 years) but with varying significance levels<sup>57</sup>. Several studies have examined the relationships between the ISM and ENSO phenomenon and/or variations in SST and sea surface pressure (SSP) in the Pacific Ocean<sup>58</sup>. This result suggests that  $\delta^{18}\text{O}_{\text{tr}}$  records multiple ENSO phenomena. Several studies<sup>59,60</sup> have pointed to the fact that the influence of the ENSO phenomenon on the ASM varies over time.

Similar influences of ENSO on the isotopic signature in tree rings were observed in North Laos<sup>61</sup>, Thailand, Indonesia<sup>62</sup>, and China<sup>63,64</sup>. However, the strength of the ENSO influence was variable throughout the study period. In Bolivia, a reduced influence of ENSO during 1950–1974 coincided with periods of lower variance in the Southern Oscillation Index. However, it was also found that the lowest correlations with Niño 4 events occurred between 1981 and 2015. There are multiple factors that make the relationship between our  $\delta^{18}\text{O}_{\text{tr}}$  and El Niño lower. One probable factor is caused by rapid traversing of the Intertropical convergent zone (ITCZ) and/or the teleconnections with the northern Atlantic thermohaline circulation, which could weaken the Asian monsoon through the air–sea connection<sup>65</sup>. Singhratna *et al.*<sup>66</sup> found that in the past decade, Pacific SSTs have had a negative relationship with the summer monsoon in Thailand, but this relationship weakened prior to 1980 due to changes in the Walker circulation over the Thailand–Indonesian region. Therefore, variations in  $\delta^{18}\text{O}_{\text{tr}}$  with El Niño periods could come from several factors and require a more in-depth analysis.

Ashok *et al.*<sup>67</sup> explained the impact of the IOD on the IM and ENSO during the period of 1958–1997, stating that the IOD and ENSO have an integral effect on the Indian summer rainfall (ISR). Whenever the ENSO–ISR correlation was low (high), the IOD–ISR relationship was high (low). However, Ashok *et al.*<sup>68,69</sup> found that the IOD is a physical mode of the tropical Indian Ocean and that the evolution of the IOD is mostly independent from the Pacific's influence<sup>70,71</sup>.

Based on the results presented in Fig. S2(A–C), SSTs in the central Pacific Ocean and Indian Ocean during the periods of 1870–2015, 1870–1942 and 1943–2015 showed that SSTs of both oceans are highly correlated with our  $\delta^{18}\text{O}_{\text{tr}}$ . Positive IOD phases occurred in 1961, 1963, 1972, 1982, 1983, 1994, 1997, 2006, and 2012. Furthermore, we found that Thailand's rainy season precipitation was below average in 1972, 1979, 1982, 1984, 1985, 1986, 1993, 1998, 1999, 2004, 2009, 2012, 2014, and 2015. Bridhikitti<sup>72</sup> investigated the connection of ENSO/IOD with Thai rainfall anomalies during the period of 1980–2011 based on instrumental data from 17 locations. He found that the effect of ENSO on summer monsoon rainfall was not obvious, but the negative (positive) IODs in October, November, and December corresponded with La Niña (El Niño) signals, which may be seen in increased (decreased) rainfall on the southeast coast during the months of December, January and February.

Severe IOD events in the summer monsoon season could affect rainfall in northern Thailand in the following year. Chansaengkrachang *et al.*<sup>73</sup> studied the time lags between IOD and rainfall over Thailand during the period of 1979–2008 based on rainfall data derived from 80 meteorological stations spread throughout Thailand. It was found that signal consistency in years of strong IOD showed an offset of approximately 11 months. This indicates that the IOD leads the rainfall by approximately two months. In addition, Hochreuther *et al.*<sup>74</sup> found positive correlations between Sikkim larch (*Larix griffithii*)  $\delta^{18}\text{O}_{\text{tr}}$  during strong positive IOD phases in southeast Tibet, when heavy rains had occurred in the western part of the Indian Ocean and less rain/drought occurred in Indonesia and Australia.

Clearly, the ISM variability is complex and related to many phenomena, such as ENSO, differences in surface temperatures in the Indian Ocean (IOD) and the difference in North Atlantic SSTs<sup>75</sup>. Our  $\delta^{18}\text{O}_{\text{tr}}$  captured the season of the ISM. Our  $\delta^{18}\text{O}_{\text{tr}}$  showed a significant positive correlation with the ENSO phenomenon. As such, the creation of a network of oxygen isotope tree-ring cellulose chronologies to cover a wider area and extend the length of  $\delta^{18}\text{O}_{\text{tr}}$  is needed and would help us to better understand long-term ASM variability and its interrelationships with other atmospheric circulation patterns and climate forcing factors. This holds particularly true for Thailand, since the currently existing tree-ring  $\delta^{18}\text{O}$  are all from the Mae Hong Son Province in Northwest Thailand. To better understand the influence of the monsoon nationwide, analyzing specimens from other areas and examining the consistency of monsoon influences over the entire country is needed. Additionally, there are good possibilities to further extend the length of the existing tree-ring  $\delta^{18}\text{O}$  chronology through the use of ancient teak wood from archaeological sites.

## Methods

**Climate condition in northwestern Thailand.** Our sampling sites are located in the Mae Hong Son province, northwestern Thailand. According to instrumental records of the nearest climate station Mae Hong Son, which is located ca. 60 km away from the study sites in northwestern Thailand, the summer monsoon climate is dominant for approximately 160 days per year during the months of May to October. During the rainy season, monthly long-term (1951–2015) average rainfall is in the range of 128–249 mm and has a mean of 193 mm, with monthly mean temperatures ranging from 20–30 °C, with a seasonal mean of 27.7 °C. Relative humidity in the rainy season is within the range of 60–90%, with a mean of 80%. During the dry season, which lasts from November to April, the number of rainy days is as low as ca. 10 days, but the only days of rain within the latter part of this season occur in March and April. Monthly mean rainfall is about 10 mm on average. The monthly mean temperature in the dry season ranges from 30–35 °C, with a mean of 30 °C. Relative humidity in the dry season is between 40–60%, with a mean of only 35% (Fig. 5). The map of Thailand is obtained from the Information Center of the Faculty of Environment and Resource Studies, Mahidol University, Thailand. Detailed in Fig. 5 is created using ARGIS10.5 software owned by the Faculty of Environment and Resource Studies, Mahidol University, Thailand.

**Tree-ring material.** In this study, the teak samples were collected in Mae Hong Son province in northwest Thailand. The seven individual study sites are located within a distance of 10–20 km and are all distributed in the natural forest. Generally, teak can grow well on well-drained soils within an elevation range of 200–800 m a.s.l.<sup>76</sup>. The samples used in this study grew at altitudes of 300–600 m a.s.l. Ring width series were measured and cross-dated in an previous study<sup>77</sup>, indicating that the last tree ring was formed in 2009. To update the stable isotope chronology, we collected additional samples from six trees in 2015. The criteria for selecting the teak samples for stable isotope analysis from the previously measured ring-width data were as follows: 1) very old tree age, 2) cross dating was successful and age determination was correct, and 3) all annual ring boundaries were clearly visible. To ensure that the re-collected samples matched the previously analyzed ring-width series, we measured and cross-dated the ring-width series from the re-collected samples, through the use of standard dendrochronological techniques. For all samples, cross-correlations were checked using the COFECHA software<sup>78</sup>. Finally, 21 living teak trees, which collectively spanned the 338-year period from AD 1678–2015, were selected for the study. Instead of using the widely applied pooling method, where individual tree-rings of identical age belonging to several individuals are mixed to save time and resources<sup>79,80</sup>, we analyzed  $\delta^{18}\text{O}$  from the individual trees separately. This was done to ensure that the isotope series from trees of the different study sites were significantly correlated and to also allow a full control of the statistical characteristics of the final mean isotope chronology over its complete length.

**Cellulose extraction.** Annual rings were cut from each core with a scalpel under a binocular microscope. Each sample was ground in a ball mill prior to extracting the  $\alpha$ -cellulose<sup>81</sup>. Alpha-cellulose was extracted following the method described by Wieloch *et al.*<sup>82</sup>. Resin, fatty acids, etheric oils, and hemicellulose were extracted with a solution of 5% NaOH for 2 hours at 60 °C, two times. Then, lignin was extracted with 7% NaClO<sub>2</sub> solution, plus 100% acetic acid for 8 hours at 60 °C, five times. For the final application, the solution should have a pH value of 4.5. The remaining hemicellulose was extracted with 17% NaOH for 2 hours at room temperature. A washing procedure with boiled deionized water was interposed for three times across the different steps. Finally, samples were treated once with 1% HCl for 5 min. at room temperature, rinsed with boiling deionized water three times and then transferred from the filter funnels into Eppendorf tubes with 1 ml deionized water.

The samples were then homogenized using an ultrasonic homogenizer and freeze dried for 72 hours in a lyophilisation unit. Approximately 300  $\mu\text{g}$  of each dried  $\alpha$ -cellulose sample were weighed and wrapped in silver foil to be processed in mass spectrometry and the  $\delta^{18}\text{O}$  was measured with an Elemental Analyzer coupled to a Delta V Advantage IRMS (Thermo Fisher), while laboratory standards were periodically interposed to test analytical replication. The  $\delta^{18}\text{O}$  values were referred from the International Standard (Vienna Standard Marine Ocean

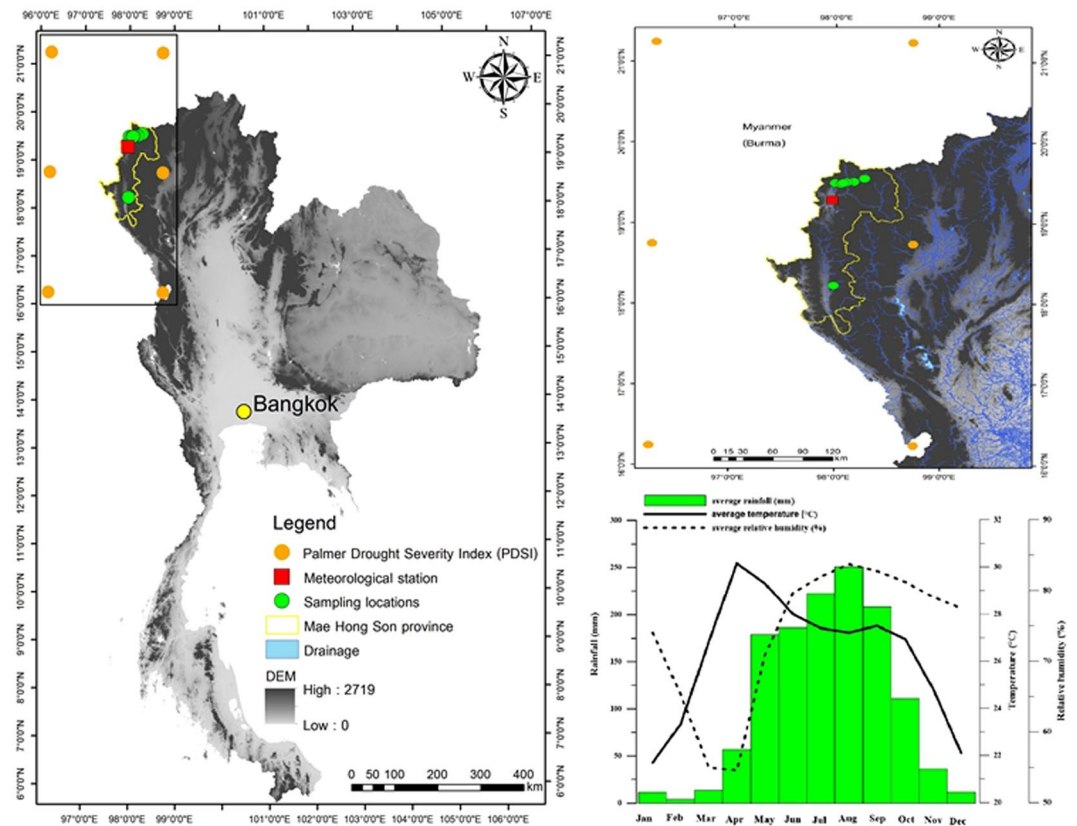


**Figure 5.** Study sites; orange circles represent six grids of PDSI, red square is the meteorological station Mae Hong Son, green circles are sampling locations, yellow line is the province boundary of Mae Hong Son, blue lines is drainage, gray scale is elevation (the left hand image), the expanded image PDSI (Top right corner) and mean (period from 1951–2015) climate conditions in Mae Hong Son Station, northwestern Thailand (Bottom right corner). The map of Thailand is obtained from the Information Center of the Faculty of Environment and Resource Studies, Mahidol University, Thailand. The six closest grid points of the PDSI, during the years 1948–2014 derived from <https://rda.ucar.edu/dataset/ds299.0/>. Maps are created using ARGIS10.5 software owner by the Faculty of Environment and Resource Studies, Mahidol University, Thailand.

Water [VSMOW]), and the overall analytical precisions was  $\pm 0.3\%$ . Cellulose extraction was conducted at the Institute of Geography, University of Erlangen-Nuremberg, Erlangen, Germany.

**Statistical analyses.** For evaluating coherence of these data, we calculated the mean inter-series correlation ( $R_{bar}$ )<sup>83</sup> and the expressed population signal, or EPS<sup>26</sup>, which indicates how well the tree-ring  $\delta^{18}O_{tr}$  estimates a theoretically infinite population. To determine the impact of the different climatic factors on  $\delta^{18}O_{tr}$ , we computed simple correlations between  $\delta^{18}O_{tr}$  and monthly means of climate data. Climate data (temperature, rainfall, and humidity) were used from the Mae Hong Son climate station (1951–2015), which was about 60 km from the study region (hereinafter will be referred to as the local climate). Additionally, CRU TS4.03 (<http://climexp.knmi.nl>) gridded temperature/precipitation data, cover Mae Hong Son province  $19^{\circ}17'17''N$ ,  $97^{\circ}57'52''E$  with a resolution  $0.5^{\circ} \times 0.5^{\circ}$  were used for correlation analyses. Henceforth, we will make use of the terminology “regional climate” for CRU-climate data. We also compared the  $\delta^{18}O$  rainfall of Bangkok (BKK, 1968–2015) and tested the similarity with various climatic indices: the Indian Monsoon (IM) Index = U850(40E–80E, 5N–15N)–U850(70E–90E, 20N–30N), the Western North Pacific Monsoon (WNPM) Index = U850(100E–130E, 5N–15N)–U850(110E–140E, 20N–30N), and the Webster and Yang Monsoon Index (WYM) Index = U850(40–110E, EQ–20N)–U200(40–110E, EQ–20N), all of which were accessed from <http://iprc.soest.hawaii.edu/users/ykaji/monsoon/definition.html>.

We analyzed the influence of different monsoon indices on our  $\delta^{18}O_{tr}$  series during the main ASM season (June–September) over the common period of 1948–2009. Furthermore, similarities with the Multivariate ENSO index (MEI) (<https://www.esrl.noaa.gov/psd/enso/mei.ext/table.ext.html>) and the Indian Ocean Dipole (IOD) model were investigated. The six closest grid points of the PDSI, during the years 1948–2014 (<https://rda.ucar.edu/dataset/ds299.0/>) were used for the evaluation of the climate sensitivity of  $\delta^{18}O_{tr}$ . Furthermore, we employed the Royal Netherlands Meteorological Institute Climate Explorer (<http://www.knmi.nl>) to examine spatial correlations between  $\delta^{18}O_{tr}$  and sea surface temperatures (SSTs), which were obtained from the National Climatic Data Centre v3b data set.

The final precipitation reconstruction was derived by linear regression, and the validity was tested by calculating Pearson’s correlation coefficients and the variance explained, adjusted variance explained, Reduction of

Error (RE), Coefficient Efficiency (CE), and Sign Test (ST)<sup>30</sup>. Precipitation over the past 338 years was then reconstructed using teak tree-ring  $\delta^{18}\text{O}$ . A Niño 4 index was used to test the stability of the teleconnection between the reconstructed precipitation and tropical pacific SSTs during the period 1870–2015. To extract cyclical variations in our records, we performed a spectral analysis on our  $\delta^{18}\text{O}_{\text{tr}}$  series using the REDFIT program for unevenly spaced time-series<sup>84</sup> (Fig. S1).

Received: 10 December 2019; Accepted: 12 May 2020;

Published online: 02 June 2020

## References

1. Loo, Y. Y., Billa, L. & Singh, A. Effect of climate change on seasonal monsoon in Asia and its impact on the variability of monsoon rainfall in Southeast Asia. *Geoscience Frontiers* **6**, 817–823, <https://doi.org/10.1016/j.gsf.2014.02.009> (2015).
2. Mendelsohn, R. The impact of climate change on agriculture in Asia. *Journal of Integrative Agriculture* **13**, 660–665 (2014).
3. Fritts, H. C. Dendroclimatology and dendroecology. *Quatern. Res.* **1**, 419–449, [https://doi.org/10.1016/0033-5894\(71\)90057-3](https://doi.org/10.1016/0033-5894(71)90057-3) (1971).
4. Wernicke, J., Bräuning, A., Rahman, M. & Islam, M. Changes in Sensitivity of Tree-Ring Widths to Climate in a Tropical Moist Forest Tree in Bangladesh. *Forests (19994907)* **9**, <https://doi.org/10.3390/f9120761> (2018).
5. Pumijumnong, N. Dendrochronologie mit Teak (*Tectona grandis* L.) in Nord-Thailand. *Jahrringbildung—Chronologiemetz—Klimasignal. Diss. Univ. Hamburg* **104** (1995).
6. Buckley, B. M., Palakit, K., Duangsathaporn, K., Sanguantham, P. & Prasomsin, P. Decadal scale droughts over northwestern Thailand over the past 448 years: links to the tropical Pacific and Indian Ocean sectors. *Climate Dynamics* **29**, 63–71, <https://doi.org/10.1007/s00382-007-0225-1> (2007).
7. D'Arrigo, R., Palmer, J., Ummenhofer, C. C., Kyaw, N. N. & Krusic, P. Three centuries of Myanmar monsoon climate variability inferred from teak tree rings. *Geophys. Res. Lett.* **38**, <https://doi.org/10.1029/2011GL049927> (2011).
8. Borgaonkar, H. P., Sikder, A., Ram, S. & Pant, G. B. El Niño and related monsoon drought signals in 523-year-long ring width records of teak (*Tectona grandis* LF) trees from south India. *Palaeogeogr., Palaeoclimatol., Palaeoecol.* **285**, 74–84, <https://doi.org/10.1016/j.palaeo.2009.10.026> (2010).
9. Ram, S., Borgaonkar, H. & Sikder, A. Tree-ring analysis of teak (*Tectona grandis* LF) in central India and its relationship with rainfall and moisture index. *Journal of earth system science* **117**, 6, <https://doi.org/10.1007/s12040-008-0058-2> (2008).
10. Evans, M. Toward forward modeling for paleoclimatic proxy signal calibration: A case study with oxygen isotopic composition of tropical woods. *Geochem. Geophys. Geosyst.* **8**, <https://doi.org/10.1029/2006GC001406> (2007).
11. Evans, M. N. & Schrag, D. P. A stable isotope-based approach to tropical dendroclimatology. *Geochim. Cosmochim. Acta* **68**, 3295–3305, <https://doi.org/10.1016/j.gca.2004.01.006> (2004).
12. Anchukaitis, K. J., Evans, M. N., Wheelwright, N. T. & Schrag, D. P. Stable isotope chronology and climate signal calibration in neotropical montane cloud forest trees. *Journal of Geophysical Research: Biogeosciences* **113**, <https://doi.org/10.1029/2007JG000613> (2008).
13. Brienen, R. J., Helle, G., Pons, T. L., Guyot, J.-L. & Gloor, M. Oxygen isotopes in tree rings are a good proxy for Amazon precipitation and El Niño–Southern Oscillation variability. *Proceedings of the National Academy of Sciences* **109**, 16957–16962, [www.pnas.org/cgi/doi/10.1073/pnas.1205977109](http://www.pnas.org/cgi/doi/10.1073/pnas.1205977109) (2012).
14. Gessler, A. *et al.* Stable isotopes in tree rings: towards a mechanistic understanding of isotope fractionation and mixing processes from the leaves to the wood. *Tree physiology* **34**, 796–818, <https://doi.org/10.1093/treephys/tpu040> (2014).
15. Young, G. H. *et al.* Age trends in tree ring growth and isotopic archives: A case study of *Pinus sylvestris* L. from northwestern Norway. *Global Biogeochem. Cycles* **25**, <https://doi.org/10.1029/2010GB003913> (2011).
16. Yakir, D. & da SL Sternberg, L. The use of stable isotopes to study ecosystem gas exchange. *Oecologia* **123**, 297–311, <https://doi.org/10.1007/s004420051016> (2000).
17. Liu, Y. *et al.* Recent enhancement of central Pacific El Niño variability relative to last eight centuries. *Nature communications* **8**, 1–8, <https://doi.org/10.1038/ncomms15386> (2017).
18. Wernicke, J. *et al.* Air mass origin signals in  $\delta^{18}\text{O}$  of tree-ring cellulose revealed by back-trajectory modeling at the monsoonal Tibetan plateau. *Int. J. Biometeorol.* **61**, 1109–1124, <https://doi.org/10.1007/s00484-016-1292-y> (2017).
19. Saurer, M. *et al.* An investigation of the common signal in tree ring stable isotope chronologies at temperate sites. *Journal of Geophysical Research: Biogeosciences* **113**, <https://doi.org/10.1029/2008JG000689> (2008).
20. Young, G. H. *et al.* Oxygen stable isotope ratios from British oak tree-rings provide a strong and consistent record of past changes in summer rainfall. *Climate Dynamics* **45**, 3609–3622, <https://doi.org/10.1007/s00382-015-2559-4> (2015).
21. Labuhn, I. *et al.* French summer droughts since 1326 CE: a reconstruction based on tree ring cellulose  $\delta^{18}\text{O}$ . *Climate of the Past* **12**, 1101–1117, <https://doi.org/10.5194/cp-12-1101-2016> (2016).
22. Buajan, S., Pumijumnong, N., Li, Q. & Liu, Y. Oxygen isotope ( $\delta^{18}\text{O}$ ) of teak tree-rings in north-west thailand. *Journal of Tropical Forest Science*, 396–405, <https://www.jstor.org/stable/43956806> (2016).
23. Schollaen, K. *et al.* Multiple tree-ring chronologies (ring width,  $\delta^{13}\text{C}$  and  $\delta^{18}\text{O}$ ) reveal dry and rainy season signals of rainfall in Indonesia. *Quaternary Science Reviews* **73**, 170–181, <https://doi.org/10.1016/j.quascirev.2013.05.018> (2013).
24. Muangsong, C., Cai, B., Pumijumnong, N., Hu, C. & Lei, G. Intra-seasonal variability of teak tree-ring cellulose  $\delta^{18}\text{O}$  from northwestern Thailand: A potential proxy of Thailand summer monsoon rainfall. *The Holocene* **26**, 1397–1405, <https://doi.org/10.1177/0959683616640045> (2016).
25. Muangsong, C., Cai, B., Pumijumnong, N., Lei, G. & Wang, F. A preliminary study on teak tree ring cellulose  $\delta^{18}\text{O}$  from northwestern Thailand: the potential for developing multiproxy records of Thailand summer monsoon variability. *Theoretical and applied climatology* **136**, 575–586, <https://doi.org/10.1007/s00704-018-2499-0> (2019).
26. Wigley, T. M., Briffa, K. R. & Jones, P. D. On the average value of correlated time series, with applications in dendroclimatology and hydrometeorology. *Journal of climate and Applied Meteorology* **23**, 201–213, doi:10.1175/1520-0450(1984)023<0201:OTAVOC>2.0.CO;2 (1984).
27. Buras, A. A comment on the expressed population signal. *Dendrochronologia* **44**, 130–132, <https://doi.org/10.1016/j.dendro.2017.03.005> (2017).
28. Enfield, D. B., Mestas-Núñez, A. M. & Trimble, P. J. The Atlantic multidecadal oscillation and its relation to rainfall and river flows in the continental US. *Geophys. Res. Lett.* **28**, 2077–2080, <https://doi.org/10.1029/2000GL012745> (2001).
29. Gupta, A. K., Das, M. & Anderson, D. M. Solar influence on the Indian summer monsoon during the Holocene. *Geophys. Res. Lett.* **32**, <https://doi.org/10.1029/2005GL022685> (2005).
30. Fritts, H. *Tree rings and climate* (Academic Press, 1976).
31. Dansgaard, W. Stable isotopes in precipitation. *Tellus* **16**, 436–468, <https://doi.org/10.3402/tellusa.v16i4.8993> (1964).
32. Pumijumnong, N., Eckstein, D. & Sass, U. Tree-ring research on *Tectona grandis* in northern Thailand. *Iawa Journal* **16**, 385–392, <https://doi.org/10.1163/22941932-90001428> (1995).

33. Le Duy, N., Heidbüchel, I., Meyer, H., Merz, B. & Apel, H. What controls the stable isotope composition of precipitation in the Mekong Delta? A model-based statistical approach. *Hydrology and Earth System Sciences* **22**, 1239–1262, <https://doi.org/10.5194/hess-22-1239-2018> (2018).
34. Cai, B. *et al.* Effects of intraseasonal variation of summer monsoon rainfall on stable isotope and growth rate of a stalagmite from northwestern Thailand. *Journal of Geophysical Research: Atmospheres* **115**, <https://doi.org/10.1029/2009JD013378> (2010).
35. Wei, Z. *et al.* Influences of large-scale convection and moisture source on monthly precipitation isotope ratios observed in Thailand, Southeast Asia. *Earth Planet. Sci. Lett.* **488**, 181–192, <https://doi.org/10.1016/j.epsl.2018.02.015> (2018).
36. Shen, H. & Poulsen, C. J. Precipitation  $\delta^{18}\text{O}$  on the Himalaya-Tibet orogeny and its relationship to surface elevation. *Clim Past* **15**, 169–187, <https://doi.org/10.5194/cp-2018-117> (2019).
37. Kumar, B. *et al.* Isotopic characteristics of Indian precipitation. *Water Resour. Res.* **46**, <https://doi.org/10.1029/2009WR008532> (2010).
38. Volland, F., Pucha, D. & Braeuning, A. Hydro-climatic variability in southern Ecuador reflected by tree-ring oxygen isotopes. *Erdkunde*, 69–82, <https://www.jstor.org/stable/24892591> (2016).
39. Managave, S. *et al.* Response of cellulose oxygen isotope values of teak trees in differing monsoon environments to monsoon rainfall. *Dendrochronologia* **29**, 89–97, <https://doi.org/10.1016/j.dendro.2010.05.002> (2011).
40. Sano, M. *et al.* Moisture source signals preserved in a 242-year tree-ring  $\delta^{18}\text{O}$  chronology in the western Himalaya. *Global Planet. Change* **157**, 73–82, <https://doi.org/10.1016/j.gloplacha.2017.08.009> (2017).
41. McCarroll, D. & Loader, N. J. Stable isotopes in tree rings. *Quaternary Science Reviews* **23**, 771–801, <https://doi.org/10.1016/j.quascirev.2003.06.017> (2004).
42. Muangsong, C. *et al.* Effect of changes in precipitation amounts and moisture sources on inter- and intra-annual stable oxygen isotope ratios ( $\delta^{18}\text{O}$ ) of teak trees from northern Thailand. *Agricultural and Forest Meteorology* **281**, 107820, <https://doi.org/10.1016/j.agrformet.2019.107820> (2020).
43. Pumijumnong, N., Muangsong, C., Buajan, S., Sano, M. & Nakatsuka, T. Climate variability over the past 100 years in Myanmar derived from tree-ring stable oxygen isotope variations in Teak. *Theoretical and Applied Climatology* **139**, 1401–1414, <https://doi.org/10.1007/s00704-019-03036-y> (2020).
44. Xu, C., Pumijumnong, N., Nakatsuka, T., Sano, M. & Li, Z. A tree-ring cellulose  $\delta^{18}\text{O}$ -based July–October precipitation reconstruction since AD 1828, northwest Thailand. *Journal of Hydrology* **529**, 433–441, <https://doi.org/10.1016/j.jhydrol.2015.02.037> (2015).
45. Xu, C., Pumijumnong, N., Nakatsuka, T., Sano, M. & Guo, Z. Inter-annual and multi-decadal variability of monsoon season rainfall in central Thailand during the period 1804–1999, as inferred from tree ring oxygen isotopes. *International Journal of Climatology* **38**, 5766–5776, <https://doi.org/10.1002/joc.5859> (2018).
46. Zhu, M., Stott, L., Buckley, B. & Yoshimura, K. 20th century seasonal moisture balance in Southeast Asian montane forests from tree cellulose  $\delta^{18}\text{O}$ . *Clim. Change* **115**, 505–517, <https://doi.org/10.1007/s10584-012-0439-z> (2012).
47. Sano, M., Xu, C. & Nakatsuka, T. A 300-year Vietnam hydroclimate and ENSO variability record reconstructed from tree ring  $\delta^{18}\text{O}$ . *Journal of Geophysical Research: Atmospheres* **117**, <https://doi.org/10.1029/2012JD017749> (2012).
48. Xu, C., Sano, M. & Nakatsuka, T. Tree ring cellulose  $\delta^{18}\text{O}$  of *Fokienia hodginsii* in northern Laos: A promising proxy to reconstruct ENSO? *Journal of Geophysical Research: Atmospheres* **116**, <https://doi.org/10.1029/2011JD016694> (2011).
49. Tan, L. *et al.* Rainfall variations in central Indo-Pacific over the past 2,700 y. *Proceedings of the National Academy of Sciences* **116**, 17201–17206, <https://doi.org/10.1073/pnas.1903167116> (2019).
50. Muangsong, C., Cai, B., Pumijumnong, N., Hu, C. & Cheng, H. An annually laminated stalagmite record of the changes in Thailand monsoon rainfall over the past 387 years and its relationship to IOD and ENSO. *Quaternary International* **349**, 90–97, <https://doi.org/10.1016/j.quaint.2014.08.037> (2014).
51. Cook, E. R. *et al.* Asian monsoon failure and megadrought during the last millennium. *Science* **328**, 486–489, <https://doi.org/10.1126/science.1185188> (2010).
52. Anderson, D. M., Overpeck, J. T. & Gupta, A. K. Increase in the Asian southwest monsoon during the past four centuries. *Science* **297**, 596–599, <https://doi.org/10.1126/science.1072881> (2002).
53. Nakamura, N. *et al.* Mode shift in the Indian Ocean climate under global warming stress. *Geophys. Res. Lett.* **36**, <https://doi.org/10.1029/2009GL040590> (2009).
54. Pratarastapornkul, T. in IOGOOS Workshop and the fifth annual meeting.
55. Malik, A. *et al.* Decadal to multi-decadal scale variability of Indian summer monsoon rainfall in the coupled ocean-atmosphere-chemistry climate model SOCOL-MPIOM. *Climate dynamics* **49**, 3551–3572, <https://doi.org/10.1007/s00382-017-3529-9> (2017).
56. Achuthavarier, D., Krishnamurthy, V., Kirtman, B. P. & Huang, B. Role of the Indian Ocean in the ENSO–Indian summer monsoon teleconnection in the NCEP Climate Forecast System. *J. Clim.* **25**, 2490–2508, <https://doi.org/10.1175/JCLI-D-11-00111.1> (2012).
57. Varikoden, H. & Babu, C. Indian summer monsoon rainfall and its relation with SST in the equatorial Atlantic and Pacific Oceans. *International Journal of Climatology* **35**, 1192–1200, <https://doi.org/10.1002/joc.4056> (2015).
58. Roy, I. & Tedeschi, R. G. Influence of ENSO on regional Indian summer monsoon precipitation—local atmospheric influences or remote influence from Pacific. *Atmosphere* **7**, 25, <https://doi.org/10.3390/atmos7020025> (2016).
59. Webster, P. J. & Yang, S. Monsoon and ENSO: Selectively interactive systems. *Quarterly Journal of the Royal Meteorological Society* **118**, 877–926, <https://doi.org/10.1002/qj.49711850705> (1992).
60. Gadgil, S., Vinayachandran, P., Francis, P. & Gadgil, S. Extremes of the Indian summer monsoon rainfall, ENSO and equatorial Indian Ocean oscillation. *Geophys. Res. Lett.* **31**, <https://doi.org/10.1029/2004GL019733> (2004).
61. Xu, C., Sano, M. & Nakatsuka, T. A 400-year record of hydroclimate variability and local ENSO history in northern Southeast Asia inferred from tree-ring  $\delta^{18}\text{O}$ . *Palaeogeogr., Palaeoclimatol., Palaeoecol.* **386**, 588–598, <https://doi.org/10.1016/j.palaeo.2013.06.025> (2013).
62. Poussart, P. F., Evans, M. N. & Schrag, D. P. Resolving seasonality in tropical trees: multi-decade, high-resolution oxygen and carbon isotope records from Indonesia and Thailand. *Earth Planet. Sci. Lett.* **218**, 301–316, [https://doi.org/10.1016/S0012-821X\(03\)00638-1](https://doi.org/10.1016/S0012-821X(03)00638-1) (2004).
63. Liu, Y. *et al.* Tree-ring stable carbon isotope-based May–July temperature reconstruction over Nanwutai, China, for the past century and its record of 20th century warming. *Quaternary Science Reviews* **93**, 67–76, <https://doi.org/10.1016/j.quascirev.2014.03.023> (2014).
64. Liu, W. *et al.* Tree-ring-based annual precipitation reconstruction in Kalaqin Inner Mongolia for the last 238 years. *Chin. Sci. Bull.* **56**, 2995–3002, <https://doi.org/10.1007/s11434-011-4706-6> (2011).
65. Sinha, A. *et al.* A 900-year (600 to 1500 AD) record of the Indian summer monsoon precipitation from the core monsoon zone of India. *Geophys. Res. Lett.* **34**, <https://doi.org/10.1029/2007GL030431> (2007).
66. Singhratna, N., Rajagopalan, B., Kumar, K. K. & Clark, M. Interannual and interdecadal variability of Thailand summer monsoon season. *J. Clim.* **18**, 1697–1708, <https://doi.org/10.1175/JCLI3364.1> (2005).
67. Ashok, K., Guan, Z. & Yamagata, T. Impact of the Indian Ocean dipole on the relationship between the Indian monsoon rainfall and ENSO. *Geophys. Res. Lett.* **28**, 4499–4502, <https://doi.org/10.1029/2001GL013294> (2001).
68. Ashok, K., Guan, Z. & Yamagata, T. A look at the relationship between the ENSO and the Indian Ocean dipole. *Journal of the Meteorological Society of Japan. Ser. II* **81**, 41–56, <https://doi.org/10.2151/jmsj.81.41> (2003).

69. Ashok, K., Guan, Z., Saji, N. & Yamagata, T. Individual and combined influences of ENSO and the Indian Ocean dipole on the Indian summer monsoon. *J. Clim.* **17**, 3141–3155, doi:10.1175/1520-0442(2004)017<3141:LACIOE>2.0.CO;2 (2004).
70. Vinayachandran, P., Saji, N. & Yamagata, T. Response of the equatorial Indian Ocean to an unusual wind event during 1994. *Geophys. Res. Lett.* **26**, 1613–1616, <https://doi.org/10.1029/1999GL900179> (1999).
71. Rao, S. A., Behera, S. K., Masumoto, Y. & Yamagata, T. Interannual subsurface variability in the tropical Indian Ocean with a special emphasis on the Indian Ocean dipole. *Deep Sea Research Part II: Topical Studies in Oceanography* **49**, 1549–1572, [https://doi.org/10.1016/S0967-0645\(01\)00158-8](https://doi.org/10.1016/S0967-0645(01)00158-8) (2002).
72. Bridhikitti, A. Connections of ENSO/IOD and aerosols with Thai rainfall anomalies and associated implications for local rainfall forecasts. *International journal of climatology* **33**, 2836–2845 (2013).
73. Chansaengkachang, K., Luadsong, A. & Ascharyapho, N. A study of the time lags of the Indian ocean dipole and rainfall over Thailand by using the cross wavelet analysis. *Arabian Journal for Science and Engineering* **40**, 215–225, <https://doi.org/10.1007/s13369-014-1480-1> (2015).
74. Hochreuther, P. *et al.* Influence of the Indian Ocean Dipole on tree-ring  $\delta^{18}O$  of monsoonal Southeast Tibet. *Clim. Change* **137**, 217–230, <https://doi.org/10.1007/s10584-016-1663-8> (2016).
75. Mölg, T., Maussion, F., Collier, E., Chiang, J. C. & Scherer, D. Prominent midlatitude circulation signature in High Asia's surface climate during monsoon. *Journal of Geophysical Research: Atmospheres* **122**(12), 702–712, <https://doi.org/10.1002/2017JD027414> (2017).
76. Kaosa-ard, A. Teak (*Tectona grandis* Linn. f) its natural distribution and related factors. *Nat. His. Bulletin Siam. Soc* **29**, 55–74 (1981).
77. Pumijumnong, N. Teak tree ring widths: Ecology and climatology research in Northwest Thailand. *Science, Technology and Development* **31**, 165–174 (2012).
78. Holmes, R. L. Computer-assisted quality control in tree-ring dating and measurement. <http://hdl.handle.net/10150/261223> (1983).
79. Leavitt, S. W. Tree-ring C–H–O isotope variability and sampling. *Sci. Total Environ.* **408**, 5244–5253, <https://doi.org/10.1016/j.scitotenv.2010.07.057> (2010).
80. Woodley, E. J. *et al.* Estimating uncertainty in pooled stable isotope time-series from tree-rings. *Chem. Geol.* **294**, 243–248, <https://doi.org/10.1016/j.chemgeo.2011.12.008> (2012).
81. Loader, N., Robertson, I., Barker, A., Switsur, V. & Waterhouse, J. An improved technique for the batch processing of small wholewood samples to  $\alpha$ -cellulose. *Chem. Geol.* **136**, 313–317, [https://doi.org/10.1016/S0009-2541\(96\)00133-7](https://doi.org/10.1016/S0009-2541(96)00133-7) (1997).
82. Wieloch, T., Helle, G., Heinrich, I., Voigt, M. & Schyma, P. A novel device for batch-wise isolation of  $\alpha$ -cellulose from small-amount wholewood samples. *Dendrochronologia* **29**, 115–117, <https://doi.org/10.1016/j.dendro.2010.08.008> (2011).
83. Cook, E. & Kairiukstis, L. *Methods of Dendrochronology: applications in the environmental sciences.* Dordrecht: Kluwer. 394 p (1990).
84. Schulz, M. & Mudelsee, M. REDFIT: estimating red-noise spectra directly from unevenly spaced paleoclimatic time series. *Computers & Geosciences* **28**, 421–426, [https://doi.org/10.1016/S0098-3004\(01\)00044-9](https://doi.org/10.1016/S0098-3004(01)00044-9) (2002).

## Acknowledgements

This study was supported by the German Academic Exchange Service (DAAD), the Thailand Science Research and Innovation (TSRI) grant nr. RDG5930014 and TSRI grant nr. RSA6280017, the National Natural Science Foundation of China (NSFC) grant nr. 41661144021 and 41272197, the National Key Research and Development Program of China grant nr. 2017YFA0603401, Innovation Research Team Fund of Fujian Normal University grant nr. IRTL1705, Mahidol University, Amnatcharoen campus grant 2016-2020, and Postdoctoral fellowship award from Mahidol University for 2018-2020. We are deeply thankful to Dr. Thomas Neal Stewart for editing and proofing the English language of this manuscript. We also thank the anonymous referees for their valuable input and critical regarding for the manuscript.

## Author contributions

N.P. collected data, conducted analysis and wrote the paper. A.B. facilitated stable isotope analysis and contributed to editing the paper, M.S. facilitated stable isotope analysis, T.N. facilitated stable isotope analysis, C.M. collected data, contributed to make figures, and revised the paper, S.B. collected data and facilitated extraction alpha cellulose.

## Competing interests

The authors declare no competing interests.

## Additional information

**Supplementary information** is available for this paper at <https://doi.org/10.1038/s41598-020-66001-0>.

**Correspondence** and requests for materials should be addressed to C.M.

**Reprints and permissions information** is available at [www.nature.com/reprints](http://www.nature.com/reprints).

**Publisher's note** Springer Nature remains neutral with regard to jurisdictional claims in published maps and institutional affiliations.



**Open Access** This article is licensed under a Creative Commons Attribution 4.0 International License, which permits use, sharing, adaptation, distribution and reproduction in any medium or format, as long as you give appropriate credit to the original author(s) and the source, provide a link to the Creative Commons license, and indicate if changes were made. The images or other third party material in this article are included in the article's Creative Commons license, unless indicated otherwise in a credit line to the material. If material is not included in the article's Creative Commons license and your intended use is not permitted by statutory regulation or exceeds the permitted use, you will need to obtain permission directly from the copyright holder. To view a copy of this license, visit <http://creativecommons.org/licenses/by/4.0/>.

© The Author(s) 2020